Journal of Thermal Analysis and Calorimetry, Vol. 96 (2009) 2, 375–382

THERMAL DEGRADATION OF CTAB IN AS-SYNTHESIZED MCM-41

J. Goworek[1*], *Agnieszka Kierys*[1], *W. Gac*[2], *Anna Borówka*[1] *and R. Kusak*[1]

[1]Department of Adsorption, Faculty of Chemistry, Maria Curie-Skłodowska University, Pl. M. Curie-Skłodowskiej 3 20-031 Lublin, Poland
[2]Department of Chemical Technology, Faculty of Chemistry, Maria Curie-Skłodowska University, Pl. M. Curie-Skłodowskiej 3 20-031 Lublin, Poland

Thermal evacuation of a surfactant template from pure siliceous MCM-41 and MCM-41 containing aluminium in hydrogen flow was investigated. Micelle templated MCM-41 were prepared using hexadecyltrimethylammonium bromide (CTAB). The products of thermal surfactant degradation outside and inside pores were identified at various temperatures using ^{13}C solid-state nuclear magnetic resonance (NMR) spectroscopy, gas chromatography coupled with mass spectrometer (GC-MS) and temperature programmed desorption coupled with mass spectrometer (TPD-MS). The GC-MS and ^{13}C MAS NMR results obtained from this study provide an insight into the mechanism of surfactant transformation during MCM-41 synthesis on molecular level.

Keywords: *CTAB, GC-MS, MAS NMR, MCM-41, template removal*

Introduction

The synthesis and properties of highly ordered mesoporous materials M41S were reported by the Mobil scientists fifteen years ago [1, 2]. The silica based MCM-41 as a member of this family of the materials attracted most attention due to its hexagonal array of uniform pores, the high surface area and high total pore volume. Although the structural properties of these mesoporous solids as well as various routes of their synthesis were extensively investigated over the last years, the processes inside the pores at subsequent stages of the preparation procedure are still under discussion. The surfactant transformations against the temperature during calcination are well recognized up to ~250°C. Above this temperature in the oxidizing atmosphere the chemical species present inside pores are transformed into carbon dioxide and water. The thermal decomposition of the surfactant template (CTAB) was studied in detail using the TPD technique [3–6]. High temperature treatment of as-synthesized MCM-41 changes additionally the concentration of the surface hydroxyls, which decreases upon calcination [7, 8]. The most commonly method used to remove the template is the calcination in air. After calcination on the silica surface remain hardly removable carbon deposits or coke [9–11].

The mechanism of the surfactant decomposition during calcination has a step-character as described by Kleitz *et al*. [12, 13]. They suggested that below 250°C 46% of the template is removed by hexadecene evaporation resulting from the Hoffman degradation and elimination of trimethylamine. Both compounds were reported earlier by Beck *et al*. [2] and Keene *et al*. [14] for MCM-41 templated by hexadecyltrimethylammonium chloride. At a relatively low temperature 250–300°C fragmentation of the alkyl chain takes also place producing shorter hydrocarbons [15, 16].

Recently Kumar *et al*. [17] carried out ^{13}C CPMAS NMR studies of the thermal decomposition of the template CTAB at 200°C. They stated the presence of N,N-dimethylhexadecylamine $CH_3(CH_2)_{15}N(CH_3)_2$ as a product of CTAB decomposition in MCM-41 surroundings.

In our previous paper [18] we demonstrated the presence of 1-hexadecene and N,N-dimethylhexadecylamine in the liquid residue that condensed at the outlet of the chromatographic column containing MCM-41 sample heated up to 250°C in hydrogen flow. Under these conditions we obtained MCM-41 silica synthesized by CTAB as a template possessing emptied pores and structural parameters similar to those of the calcined sample. Moreover, most of the surface silanols were preserved, and their concentration was much higher than for the calcined sample.

In the present paper the results of similar experiments for silica and silica–aluminium of the MCM-41 type are reported. The aim of this study was to give some information on the chemical processes involved in the surfactant removal in non-oxidizing atmosphere. An additional aim of the present paper was to test how aluminium incorporated into the framework of MCM-41 mesoporous materials influences the re-

* Author for correspondence: jgoworek@hermes.umcs.lublin.pl

1388–6150/$20.00

Akadémiai Kiadó, Budapest, Hungary
Springer, Dordrecht, The Netherlands

moval of surfactant degradation products and chemical processes during heat treatment. The surfactant degradation products in different surroundings were investigated using gas chromatography coupled with mass spectrometry (GC-MS), temperature programmed desorption coupled with mass spectrometry (TPD-MS) and solid-state ^{13}C MAS NMR spectroscopy.

Experimental

Sample preparation

The investigated silica materials were synthesized using hexadecyltrimethylammonium bromide (CTAB, 96%, Fluka) and tetraethoxysilane (TEOS, 98%, Fluka) as a silica source and aluminum sulphate ($Al_2SO_4 \cdot 18H_2O$) as an aluminium source. The detailed procedure of the preparation was described previously for MCM-41 [19] and Al–MCM-41 [20]. The as-synthesized samples were dried at 90°C in order to preserve the micellar template in the pores. The initial samples were denoted as MCM-41-AS and 50Al–MCM-41-AS (n_{Si}/n_{Al}=50) and 15Al–MCM-41-AS (n_{Si}/n_{Al}=15). Prior to the experiment a part of raw MCM-41, 50Al–MCM-41 and 15Al–MCM-41 was calcined at 550°C for 8 h and then heated at 550°C in an oxygen stream in order to complete the removal of the carbon deposits remaining after calcination. Next, samples were prepared by heating as-synthesized samples at 150 and 300°C for 10 h in a hydrogen stream in order to avoid pyrolysis of the organic template. The samples were denoted: calcined and whitened as MCM-41-OX, 50Al–MCM-41-OX, 15Al–MCM-41-OX, thermally treated at 150°C in hydrogen as MCM-41-150, 50Al–MCM-41-150, 15Al–MCM-41-150 and thermally treated in hydrogen at 300°C as MCM-41-300, 50Al–MCM-41-300 and 15Al–MCM-41-300.

Methods

Temperature programming studies were performed in the system coupled on-line with mass spectrometer (MS) HAL201RC (HIDEN Analytical) by a heated stainless steel capillary. Samples (0.05 g) were placed on quartz wool (RESTEK #20790) inside the flow glass reactor (i.d.=10 mm). Initially, the samples were washed at room temperature in helium (99.999% BOC Gazy) for 30 min and then in pure hydrogen (BOC Gazy) for 5 min. A temperature controller maintained the reactor temperature within 1°C and provided linear temperature programming. The samples were then heated with linear temperature programming 10°C min^{-1} up to 450°C in a hydrogen flow. With the help of mass spectrometer were recorded the changes of signal of selected ions, e.g.: m/z=2, 16, 17, 18, 26, 30, 32, 43, 44, 55, 58.

Nitrogen adsorption measurements were carried out using a volumetric adsorption analyzer ASAP 2405 (Micromeritics, Norcros, GA). The specific surface areas, S_{BET}, were calculated using the BET method for the adsorption data in a relative pressure range p/p_0 from 0.05 to 0.25. Pore size and pore size distribution were determined using the Barrett–Joyner–Halenda (BJH) [21] and Kruk–Jaroniec–Sayari (KJS) [22, 23] procedures.

GC-MS analysis was performed using gas chromatograph combined with a mass spectrometer GCQ (Thermo-Finningan, USA) equipped with two different capillary columns: a high temperature one MTX-1 (Resteck) of 0.25 mm ID and 15 m length with linear temperature programming 15°C min^{-1} up to 370°C in a helium flow of 0.50 mL min^{-1}; the other a low temperature one RTx-5 (Resteck) of 0.18 mm ID and 20 m length with the linear temperature programming 15°C min^{-1} up to 320°C in a helium flow of 0.50 mL min^{-1}. MS analysis was realized using electron ionization 70 V within 35–400 m/z.

X-ray powder diffraction (XRD) patterns were measured on Dyfractometer HZG 4AZ (Germany) using CuK_α radiation. X-ray patterns were obtained by measuring the number of impulses within a given angle over 10 s. The measurements were taken of every 0.02°.

The ^{13}C CP MAS NMR and ^{27}Al HPD NMR spectra of the solid samples were carried out on a Bruker Avance-300 spectrometer. The ^{13}C CP MAS spectra were recorded at 75.52 MHz. The carbon chemical shifts are given in ppm and referenced to the high frequency peak of glicine on TMS scale. About 300–8000 scans were applied until a satisfactory signal-to-noise ratio was achieved. In experiments 4 mm circonia rotors spun at 8 kHz were used. ^{27}Al-single pulse excitation with high power proton decoupling (HPD) spectra were recorded at 78.26 MHz~2100 scans.

The elemental analysis of the investigated samples was performed using a CHN analyzer (Perkin-Elmer CHN 2400).

Results and discussion

MCM-41 and Al-MCM-41 – structural characterization

Low-temperature nitrogen adsorption

Figure 1 shows the nitrogen adsorption/desorption isotherms measured for samples treated at different temperatures in hydrogen flow and additionally for the samples after calcination. The nitrogen adsorption for the samples heated at 150°C is relatively low and in-

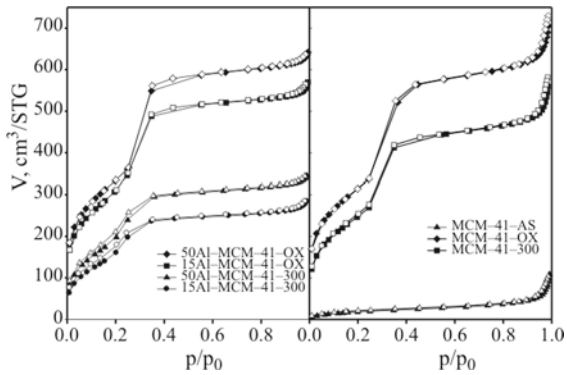

Fig. 1 Nitrogen adsorption/desorption isotherms at –195°C for the samples under study. Filled points – adsorption, open points – desorption

creases for the samples heated at 300°C, which suggests progressive pore emptying. The degree of the template evacuation is higher for pure siliceous MCM-41 as compared to Al–MCM-41. In the latter case a substantial part of pores was probably still filled with surfactant molecules or other products of surfactant transformation. The specific surface areas, S_{BET}, the total pore volumes, V_p, and the pore dimensions, D_p, derived from the nitrogen desorption data are gathered in Table 1. The shape of the nitrogen isotherms changed from type I to type IV with temperature increase. Simultaneously, the specific surface area BET of the sample as well as the total pore volume calculated from the single adsorption point at $p/p_0 \approx 0.9$ increase. The characteristic condensation steps at $p/p_0 \approx 0.4$ corresponding to the regular mesopores for the MCM-41 and Al–MCM-41 calcined and additionally whitened by prolonged heating at 550°C in O_2 is observed. However, these steps are wider and the steepest segment of the isotherm is shifted towards the smaller relative pressure for the same samples evacuated at 300°C. It means that pore emptying takes place along regular pores. The effective pore dimensions are lower than in the calcined sample and represent the emptied core of the pore. In this case free space created after a partial template removal can be assumed as the pore core. The pore dimensions presented in Table 1 confirm this suggestion.

The extent of nitrogen adsorption and the values of the parameters characterizing the pore structure are lower for all investigated samples evacuated at 300°C than for those calcined. However, it is clearly visible that the degree of the template evacuation is higher for pure siliceous MCM-41. It should be noted that nitrogen adsorption on the samples with partially filled pores is not reversible in the whole relative pressure range. This effect was observed for MCM-41 by Keene [14] and reported in our previous paper [18]. The unusual hysteresis is probably connected with restricted nitrogen diffusion between the surfactant chains present in the pores. Similar phenomena occur in the adsorption on polymeric and swelling adsorbents [24].

XRD

All investigated samples exhibit the XRD patterns characteristic of the MCM-41 phase. For illustrative purposes Fig. 2 shows the dyfractograms for 15Al–MCM-41 and 50Al–MCM-41. The three peaks observed at low diffraction angles represent (100), (110) and (200) reflections which are characteristic of the hexagonal structure of MCM-41. The XRD patterns show decrease in the peak intensity and resolution as the aluminum concentration in the sample increases. The temperature increase does not improve the intensity of the reflections. It suggests that even at a higher temperature pores are partially filled with organic species. The total pore emptying should lead to intensity increase of the XRD peaks due to a better electronic contrast between the silica framework and the pore interior. The $d(100)$ spacing values derived from the location of the peak (100), using Bragg law, are collected in column V of Table 1. The observed gradual decrease of $d(100)$ with increasing temperature is a result of shrinkage of the silica or silica/aluminium network [12].

The products of CTAB degradation in H_2

Pure CTAB

The composition of the condensate obtained from the sample containing pure surfactant CTAB mixed with

Table 1 Structural parameters obtained from the nitrogen adsorption data and X-ray diffraction for MCM-41 samples investigated

Sample	S_{BET}/m^2 g^{-1}	V_p/cm^3 g^{-1}	D_p^{BJH}/nm	d_{100}/nm	D_p^{KIS}/nm
MCM-41-AS	68	0.13	–	4.09	–
MCM-41-300	890	0.84	2.24	3.98	3.55
MCM-41-OX	1126	1.07	2.29	3.84	3.75
15Al–MCM-41-OX	1100	0.86	2.32	3.77	3.37
15Al–MCM-41-150	27	0.04	–	4.05	–
15Al–MCM-41-300	578	0.43	2.22	3.91	2.99
50Al–MCM-41-OX	1193	0.96	2.33	3.65	3.43
50Al–MCM-41-150	43	0.06	–	3.98	–
50Al–MCM-41-300	710	0.53	2.23	3.78	3.15

macroporous silica gel Si-1000 and processed at 150 and 300°C in hydrogen flow is shown in Fig. 3. Trimethylamine is formed at 150°C. The condensate from the sample contains mainly 1-hexadecene and N,N-dimethylhexadecylamine. However, the composition of the liquid/solid condensate at the 300°C is more complex. As it is seen there are three peaks which can be ascribed to hexadecene isomers and two amines: N,N-dihexadecylamine, M_w=465 and N,N,N-trihexadecylamine M_w=689.

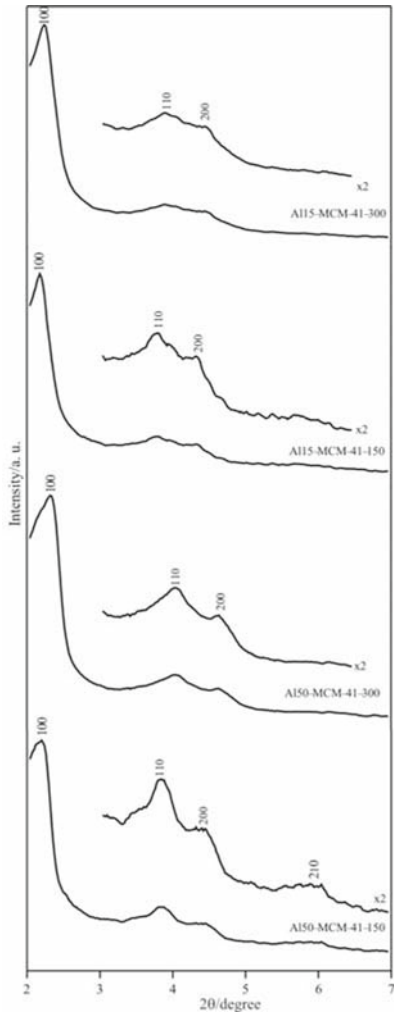

Fig. 2 X-ray powder diffraction patterns for Al–MCM-41 materials investigated

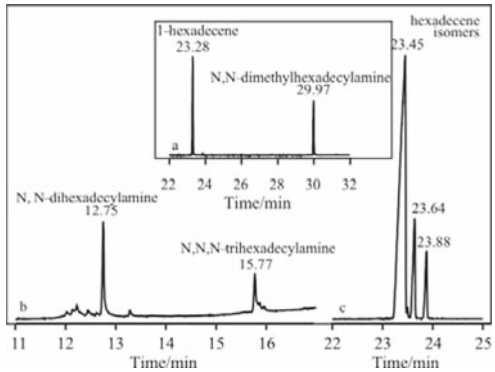

Fig. 3 GC-MS analysis of CTAB degradation products; a – 150°C (Resteck MTX-1), b – 300°C (Resteck MTX-1) and c – 300°C (Resteck RTx-5)

CTAB inside pores of MCM-41 and Al–MCM-41

The products of CTAB degradation, entrapped inside the pores of the raw materials MCM-41 and Al–MCM-41 were analyzed using TPD-MS (volatile species) and for larger molecules (analysis of condensate and not evacuated organics) using GC-MS and ^{13}C MAS NMR.

TPD-MS

The TPD-MS spectra of the MCM-41 series of the samples are shown in Fig. 4. The two main products are formed at lower temperatures. One can observe a water loss within the temperature range 20–150°C (Fig. 4a). This process exhibits a two-step mechanism

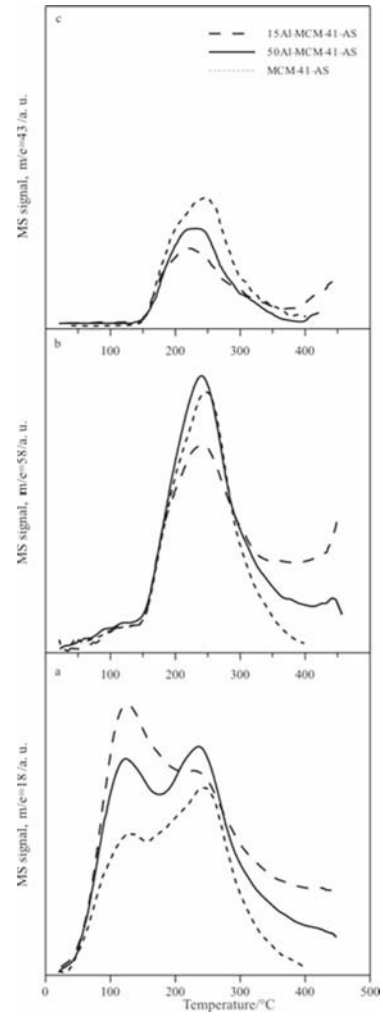

Fig. 4 TPD-MS of a – water, b – 1-hexadecene and c – trimethylamine for investigated samples

confirmed by the presence of two peaks on the TPD spectra. The proportion of these peaks changes for samples of different Si/Al ratios. The peak at lower temperature increases for samples containing aluminium. Simultaneously, for the same samples the loss of water at higher temperatures decreases. The presented results may suggest that a sample richer in aluminium contains a higher amount of physically adsorbed water. According to Lin *et al*. [25] the presence of Al may disturb the ratio of various surface silanols or change the degree of the framework condensation. Hence the peak representing desorption of weakly held water increases with Al content increase in the MCM-41 sample. Moreover, the FTIR spectra measurement of using the photoacoustic detector (PAS) for aluminium–silica samples exhibits a more intensive band corresponding to the water adsorbed in the 3700–3000 cm^{-1} frequency region in comparison to the pure as-synthesized siliceous MCM-41 [26].

As can be expected, trimethylamine is another product of the template degradation at lower temperatures. The formation of trimethylamine is accompanied by parallel production of 1-hexadecene and N,N-dimethylhexadecylamine [14, 17, 18]. The curves representing the dependence of the amount of trimethylamine formed against the temperature are shown in Fig. 4b. Their shape is differentiated for silica and silica/aluminium samples. In the case of siliceous MCM-41 an intensive release of trimethylamine is observed within the temperature range 200–300°C, and then desorption continuously decreases; its maximum is observed in the same temperature range for silica–aluminium MCM-41 samples. However, amine desorption increases again above 400°C. It may suggests that CTAB molecules or its non-ionic form N,N-dimethylhexadecylamine are strongly adsorbed on MCM-41 containing aluminium. Two maxima at ~250 and above 400°C observed on the temperature-programmed desorption curves indicate a strong adsorption of amine species at Brönsted acid, and a stronger at Lewis acid site, respectively. As reported in many papers, the concentration of Lewis and Brönsted acid sites is relatively high in the Al–MCM-41 samples obtained by both post-synthesis modifications of MCM-41 (lower acidity) and Al–MCM-41 material with aluminum introduced during the synthesis (higher acidity) [27–29]. Moreover, desorption of pyridine from MCM-41 (n_{Si}/n_{Al}=20) exhibits also a bimodal character with maxima at 300 and 650°C, as reported in [30].

Figure 7b shows ^{27}Al NMR spectra for 15Al–MCM-41-150 and 15Al–MCM-41-300. The ^{27}Al NMR spectra of Al-containing samples practically have only one peak at ~51 ppm [31]. The chemical shift is consistent with the amount of aluminum incorporated in the silica framework with tetrahedral coordination. Upon calcination a new peak usually appears at ~0 ppm besides the still existing peak at 51 ppm. This indicates a small aluminum fraction removed from the framework. A weak dealumination is also observed in the case of Al containing samples thermally treated at 300°C in hydrogen, which is confirmed by the appearance of an additional peak at about –3.0 ppm. The dealumination does not influence substantially the acidity of the silica–aluminium surface.

The mesoporous 15Al–MCM-41 has the largest number of strong adsorption sites for amine, which correlates reasonably with worsening pore emptying for Al–MCM-41 in comparison to pure siliceous MCM-41 material. This effect is consistent with TPD experiments. One can assume that at 300°C the structure of CTAB or N,N-dimethylhexadecylamine remains, at least in part, intact and both these components have been strongly adsorbed on the silica–aluminium surface. A part of CTAB molecules is desorbed and transformed into various chemical species – mainly trimethylamine and 1-hexadecene below 400°C as evidenced by TPD-MS analysis. However, further thermal degradation of these species takes place at a higher temperature, which is confirmed by 1-hexadecene release above 400°C (Fig. 4c). Simultaneous appearance of a large amount of trimethylamine at the same temperature may be caused by elimination of amine as well as desorption of readsorbed trimethylamine formed at lower temperatures.

It should be stressed that the location of the desorption maxima of surfactant amine on the temperature axis is not precisely determined and depends on the heating rate applied in the TPD experiment. Usually, when the heating rate is high (as in our case) the maximum representing the given process is shifted to higher temperatures. The liberation of trimethylamine and 1-hexadecene is related probably to the moment of desorption of CTAB and N,N-dimethylhexadecylamine. Amine molecules bounded to the surface are relatively stable and can be transformed only after desorption. The total desorption of amine species requires higher and higher temperatures.

In general one can say that partial decomposition of the CTA^+ cationic surfactant into electrically neutral N,N-dimethyhexadecylamine is an easy process. In [32] amine was detected on the basis of the ^{13}C NMR spectra even at 165°C in the mother liquid during synthesis of MCM-41. The formation of the amine in the reacting mixture may cause increase of the micelle diameter and consequently of the pore diameter of the final silica material. Thus, N,N-dimethylhexadecylamine may be assumed as expander of the micellar template [33]. In our previous paper we observed the formation of N,N-dimethylhexadecylamine and 1-hexadecene in pores of as-synthesized MCM-41 at temperatures slightly higher than 110°C [18].

GC-MS analysis of the condensate outside pores

The GC chromatograms of the condensates gathered from over the silica and the silica/aluminium samples at 150 and 300°C are shown in Figs 5 and 6. The GC analysis of the liquid/solid condensate for samples treated at 150°C indicates the presence of two main products i.e. 1-hexadecene and N,N-dimethylhexadecylamine for both 15Al–MCM-41-150 and 50Al–MCM-41-150 silica-aluminium samples (Fig. 5a). The same products are detected for pure siliceous MCM-41 and CTAB at this treatment temperature [18]. Further thermal treatment of MCM-41 samples at a higher temperature leads to diversification of the chemical species.

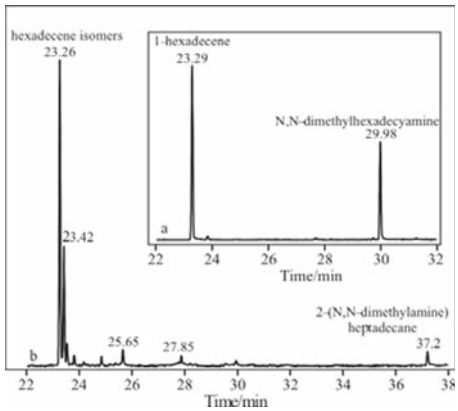

Fig. 5 GC-MS analysis of the surfactant degradation products for a – 15Al–MCM-41-150 and MCM-41-150 (Resteck RTx-5) and b – MCM-41-300 (Resteck RTx-5)

The condensate composition for pure siliceous MCM-41 and MCM-41 containing aluminium treated at 300°C is quite different (Figs 5b and 6). 1-hexadecene is the dominant peak for MCM-41-300. Moreover, a small amount of 2-(N,N-dimethylamine)heptadecane is also detected. Some traces of heavy chemical species of M_w>400 are detectable, but it is not possible to identify them. These large molecules do not represent the amines produced during thermal analysis of pure CTAB. In the case of 15Al–MCM-41-300 one can observe the presence of *n*-hexadecene isomers, *n*-heptadecene and *n*-octadecene isomers and N,N-dimethylhexadecylamine. These results indicate that the presence of aluminium causes a strong isomerization of *n*-hexadecene and partial transformation of unsaturated hydrocarbons into other members of the homologous series. The amount of encapsulated aluminium slightly influences the proportion of the obtained products. The diversity of the registered products in the condensate testifies a more complex surfactant degradation for the 15Al–MCM-41-300. In this case cracking the hydrocarbons chains should be taken into account. Catalytic activity of Al–MCM-41 in cracking

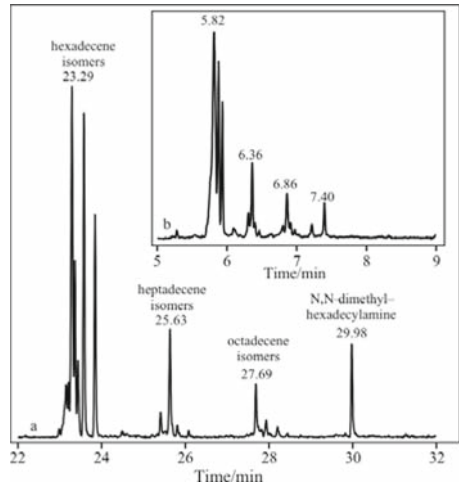

Fig. 6 GC-MS analysis of surfactant degradation products for 15Al–MCM-41-300 sample, a – column RTx-5 and b – column MTX-1

parafins and olefins was earlier reported, among other things, in [34–36].

It is hard to explain the reaction mechanism leading to the formation of higher members of the homologous series of olefins. In the case of thermal degradation of parafins C_1 and C_2 species are produced besides not branched-chain olefins. Moreover, as secondary products larger olefins and aromatics are produced [37]. Under the same conditions *n*-olefins exhibit double-bond isomerization. However, catalytic cracking of *n*-olefins in the presence of Brönsted and Lewis acid sites involves the formation of skeletal isomers as well as double-bond isomers. 1-hexadecene is mainly formed for silica and aluminium–silica samples below 250°C. N-hexadecene double-bond isomers as well as *n*-heptadecene and *n*-octadecene isomers appear at a higher temperature for aluminated samples. Thus, one can assume that both types of isomerization take place simultaneously.

It should be stressed that chemical species of a lower boiling point are not present in our condensate due to their high volatility. It follows from GC-MS analysis that the presence of *n*-alkenes in the condensate is most probable, but the formation of methyl-branched hydrocarbons is also possible. However, detection of these isomers on the basis of the of presented data is difficult.

^{13}C MAS NMR of residuals in pores

An important question is – what chemical species are present in the MCM-41 materials after thermal treatment when a part of the surfactant is evacuated? At first the character of the chemical species remaining in pores after heat treatment at 300°C was investigated by ^{13}C CPMAS NMR experiments. Figure 7a shows the ^{13}C NMR spectra for MCM-41-300,

Table 2 Elemental analysis of MCM-41 samples investigated

Sample	Elemental analysis/mass%		
	C	H	N
15Al–MCM-41-AS	31.59	6.47	1.59
15Al–MCM-41-150	30.56	6.26	1.55
15Al–MCM-41-300	15.96	3.05	0.21
MCM-41-AS	31.86	6.63	1.94
MCM-41-300	11.57	2.12	0.10
MCM-41-OX	2.28	1.20	0.11

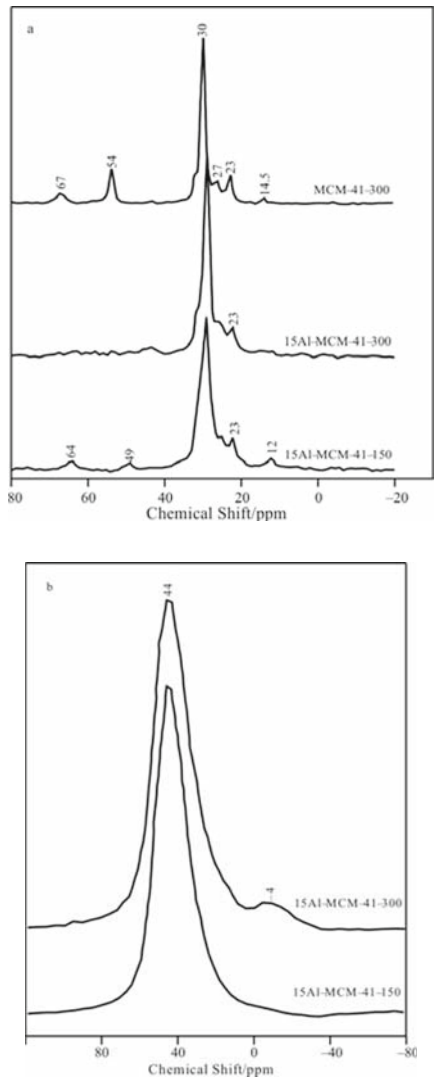

Fig. 7 The MAS NMR spectra of investigated samples; a – ^{13}C MAS NMR spectra, b – ^{27}Al MAS NMR spectra

15Al–MCM-41-300 and 15Al–MCM-41-150. The MAS NMR results are similar to those obtained elsewhere [17, 38]. The carbons in surfactant molecules are usually numbered as follows:

$$\overset{17}{CH_3}–\overset{16}{CH_2}–\overset{15}{CH_2}–(\overset{14–4}{CH_2})_{11}–\overset{3}{CH_2}–\overset{2}{CH_2}–\overset{}{N}–(\overset{1}{CH_3})_3$$

Resonances appearing at 32, 30, 27 and 23 ppm caused by C15, C4–C14, C3 and C16 are visible for all investigated samples [20, 38]. Moreover, the signals at 67 ppm (C2), 54 ppm (C1) and 14.5 ppm (C17) are observed for siliceous MCM-41-300 and 15Al–MCM-41-150 samples. Surprisingly, the resonances corresponding to carbon atoms C1, C2 and C17 practically disappear for 15Al–MCM-41-300 sample after thermal treatment at 300°C in hydrogen. The loss of the 64 and 49 ppm peaks may be due to the formation of alkene and N,N-dimethylhexadecylamine desorption as suggested by gas analysis. The ^{13}C MAS NMR spectra confirm the increase of pore emptying at increasing temperature i.e. lowering intensities of both NMR peaks after thermal treatment at higher temperature. These results are besides corroborated by the elemental analysis which confirms the template contamination decrease for samples treated at 300°C and the difference between the amounts of the remainder for pure silica sample and silica–aluminium sample (Table 2). However, as it was mentioned earlier a part of pores remains filled with organic species for both types of MCM-41 treated at 300°C in hydrogen.

Conclusions

A detailed study of template degradation in mesoporous silica and the silica–aluminium materials was carried out using the TPD-MS, GC-MS and NMR techniques. Processing the as-synthesized MCM-41 mesoporous materials prepared with CTAB as a template at various temperatures in hydrogen flow leads to the formation of different chemical species representing transformed forms of the surfactant molecules. The investigations showed the degree of CTAB transformation and the type of the produced compounds to be different for different framework composition. Trimethylamine is formed starting from relatively low temperatures for all investigated samples. 1-hexadecane and N,N-dimethylhexadecylamine appear at 150°C outside pores. Isomerization of *n*-hexadecene and production of *n*-hexadecene homologues take place in the case of aluminated samples at 300°C in hydrogen. The GC-MS analysis

and ^{13}C MAS NMR spectra showed CTAB to be efficiently decomposed during the heat treatment, whereas the structure of N,N-dimethylhexadecylamine remained intact up to 300°C. The efficiency of template removal is higher for pure siliceous MCM-41 as compared to aluminium containing MCM-41. N,N-dimethylhexadecylamine interaction with the MCM-41 surface is one of the most important factors determining the extent of surfactant removal at all temperatures used. The major part of the surfactant was removed by thermal decomposition. However, trimethylamine and N,N-dimethylhexadecylamine were strongly adsorbed on aluminated MCM-41. The predominant role in adsorption of these species is played by the Lewis and Brönsted acid sites present on the MCM-41 surface. The composition of the formed substances depends on the type of the mesophase and is more complex for MCM-41 containing aluminium.

The presented results illustrate the complexity of the template transformations under various conditions. These results may be useful for modeling the synthesis procedure of micelle templated materials.

References

1 C. T. Kresge, M. E. Leonowicz, W. J. Roth, J. C. Vartuli and J. S. Beck, Nature, 359 (1992) 710.
2 J. S. Beck, J. C. Vartuli, W. J. Roth, M. E. Leonowicz, C. T. Kresge, K. D. Schmitt, C. T.-W. Chu, D. H. Olson, E. W. Sheppard, S. B. McCullen, J. B. Higgins and J. L. Schlenker, J. Am. Chem. Soc., 114 (1992) 10834.
3 S. A. Araujo, M. Ionashiro, V. J. Fernandes Jr. and A. S. Araujo, J. Therm. Anal. Cal., 64 (2001) 801.
4 R. Denoyel, M. T. J. Keene, P. L. Llewellyn and J. Rouquerol, J. Therm. Anal. Cal., 56 (1999) 261.
5 R. Zaleski, J. Wawryszczuk, A. Borówka, J. Goworek and T. Goworek, Micropor. Mesopor. Mater., 62 (2003) 47.
6 M. J. B. Souza, A. O. S. Silva, J. M. F. B. Aquino, V. J. Fernandes Jr. and A. S. Araujo, J. Therm. Anal. Cal., 75 (2004) 693.
7 T. Mori, Y. Kuroda, Y. Yoshikawa, M. Nagao and S. Kiitaka, Langmuir, 18 (2002) 1595.
8 S. Ek, A. Root, M. Peussa and L. Niinisto, Thermochim. Acta, 379 (2001) 201.
9 P. L. Llewellyn, Y. Grillet, J. Rouquerol, C. Martin and J.-P. Coulomb, Surf. Sci., 352–354 (1996) 468.
10 M. J. Hudson and P. Trens, Characterization of Porous Solids V, Studies in Surface and Catalysis, K. K. Unger, *et al*., Eds, Vol. 128, The Royal Society of Chemistry, 2000, p. 505.
11 J. Ryczkowski, J. Goworek, W. Gac, S. Pasieczna and T. Borowiecki, Thermochim. Acta, 434 (2005) 2.
12 F. Kleitz, W. Schmidt and F. Schüth, Micropor. Mesopor. Mater., 44–45 (2001) 95.
13 F. Kleitz, W. Schmidt and F. Schüth, Micropor. Mesopor. Mater., 65 (2003) 1.
14 M. T. Keene, R. D. M. Gougeon, R. Denoyel, R. K. Harris, J. Rouquerol and P. L. Llewellyn, J. Mater. Chem., 9 (1999) 2843.
15 J. Wawryszczuk, J. Goworek, R. Zaleski and T. Goworek, Langmuir, 19 (2003) 2599.
16 R. Zaleski, J. Wawryszczuk, J. Goworek, A. Borówka and T. Goworek, J. Colloid Interface Sci., 262 (2003) 466.
17 R. Kumar, H.-T. Chen, J. L. V. Escoto, V. S.-Y. Lin and M. Pruski, Chem. Mater., 18 (2006) 4319.
18 J. Goworek, A. Kierys and R. Kusak, Micropor. Mesopor. Mater., 98 (2007) 242.
19 M. Grün, K. K. Unger, A. Matsumoto and K. Tsutsumi, B. McEnaney, J. T. Mays, J. Rouquerol, F. Rodriguez-Reinoso, K. S. W. Sing and K. K. Unger, Eds, Characterization of Porous Solids IV, The Royal Society of Chemistry, London 1997, p. 81.
20 M. M. L. Ribeiro Carrott, F. L. Conceição, J. M. Lopes, P. J. M. Carrott, C. Bernardes, J. Rocha and F. Ramôa Ribeiro, Micropor. Mesopor. Mater., 92 (2006) 270.
21 E. P. Barrett, L. G. Joyner and P. P. Halenda, J. Am. Chem. Soc., 73 (1951) 373.
22 M. Kruk, M. Jaroniec and A. Sayari, J. Phys. Chem. B, 101 (1997) 583.
23 M. Kruk and M. Jaroniec, Chem. Mater., 13 (2001) 3169.
24 J. Goworek, A. Deryło-Marczewska, W. Stefaniak, W. Zgrajka and R. Kusak, Mater. Chem. Phys., 77 (2002) 276.
25 W. Lin, Q. Cai, W. Pang, Y. Yue and B. Zou, Micropor. Mesopor. Mater., 33 (1999) 187.
26 A. Kierys, S. Pasieczna-Patkowska, J. Ryczkowski, A. Borówka and J. Goworek, The European Physical Journal - Special Topics, 154 (2008) 335.
27 A. Jentys, K. Kleestorfer and H. Vinek, Micropor. Mesopor. Mater., 27 (1999) 321.
28 M. J. B. Souza, A. O. S. Silva, V. J. Fernandes Jr. and A. S. Araujo, J. Therm. Anal. Cal., 79 (2005) 425.
29 A. Araujo, V. Fernandes and S. Verissimo, J. Therm. Anal. Cal., 59 (2000) 649.
30 M. Hunger, U. Schenk, M. Breuninger, R. Gläser and J. Weitkamp, Micropor. Mesopor. Mater., 27 (1999) 261.
31 R. Ryoo, C. H. Ko and R. F. Howe, Chem. Mater., 9 (1997) 1607.
32 Ch.-F. Cheng, W. Zhou and J. Klinowski, Chem. Phys. Lett., 263 (1996) 247.
33 A. Sayari, Y. Yang, M. Kruk and M. Jaroniec, J. Phys. Chem. B, 103 (1999) 3651.
34 A. Liepold, K. Roos, W. Reschetilowski, A. D. Esculcas, J. Roche, A. Philippow and A. W. Anderson, J. Chem. Soc. Faraday Trans., 92 (1996) 4623.
35 A. Corma and A. Martinez, Handbook of Porous Solids, F. Schüth, K. S. W. Sing and J. Weitkamp, Eds, Wiley-VCH, Weinheim 2002, p. 2825.
36 G. Leclercq, A. El Gharbi, L. Gengembre, T. Řomero, L. Leclercq and S. Pietrzyk, J. Catal., 148 (1994) 550.
37 G. R. Bamwenda, Y. X. Zhao and B. W. Wojciechowski, J. Catal., 148 (1994) 595.
38 L.-Q. Wang, J. Liu, G. J. Exarhos and B. C. Bunker, Langmuir, 12 (1996) 2663.

Received: February 5, 2008
Accepted: February 17, 2009
Online First: April 13, 2009

DOI: 10.1007/s10973-008-9055-6